Chapter 1

Numerical Simulation in Microforming for Very Small Metal Elements

Krzysztof Mogielnicki

Additional information is available at the end of the chapter

http://dx.doi.org/10.5772/64275

Abstract

Microforming is a technology of very small metal elements production, which are required as a parts for many industrial products resulting from microtechnology. This chapter gives a review of the state-of-the-art microforming of metals and its numerical simulations. Phenomena occurring in the miniaturization of microbulk-forming technologies are described. The main problems in microforming are size effects, which have physical and structural sources and directly affect the material flow mechanics in microscale. Size effects must be taken into account in all areas of the forming process chain, demanding new solutions, especially in workpiece structure and die surface numerical modeling.

Keywords: microforming, size effects, numerical simulation

1. Introduction

Trend of miniaturization of everyday devices increases industry demand for efficient production of miniature parts. Machining production technologies of small-dimension elements by turning, milling, and polishing are well known for a long time. However, these methods are not efficient enough for the great demand for small and handy devices. This makes engineers to search for new methods of microelements manufacturing or to adapt traditional ones for the requirements of miniaturization.

Microforming is an adopted technology of production of small parts by metal forming. This process is characterized by good productivity, high dimensions accuracy, proper surface smoothness, high material usage, and good mechanical properties of manufactured items, which makes it a good alternative to machining. Excepting benefits, microforming also brings some limitations, for example, limited forming possibilities of deformed materials or narrow shapes of obtained elements. Approaches of microforming methods are presented in **Figure 1**.

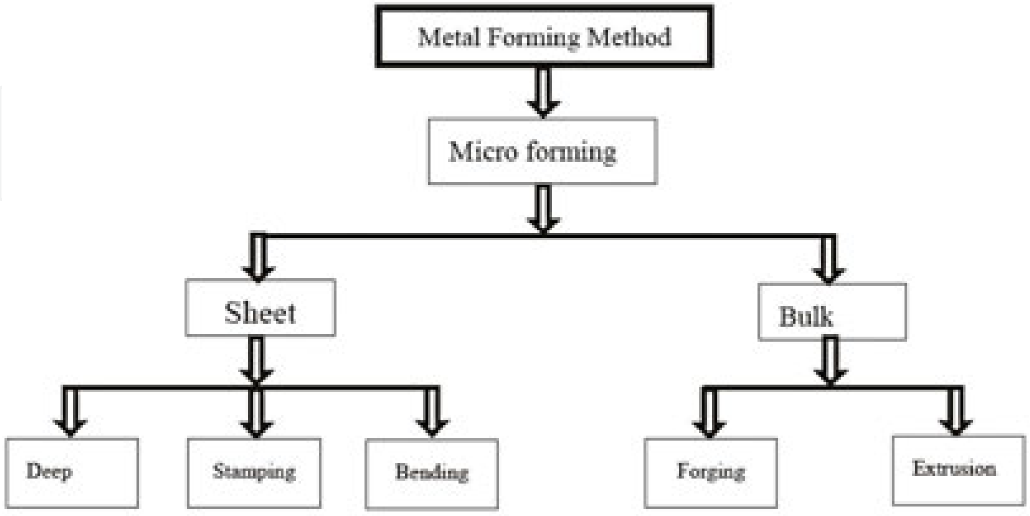

Figure 1. Microforming methods [1].

Comparing microforming to traditional forming process, it is obvious that while going to a microscale some process parameters, such as grain size or surface structure, keep constant [2]. Relationships between the dimensions of treated items and morfometric parameters of their microstructure and surface geometry, in billets as well as in tools, are different in macro- and microscale. This leads to the formation of the size effect phenomenon. In the available technological knowledge relating to conventional macroscale forming methods, presence of size effects does not permit direct application into microforming of metals [3–6]. Microforming is defined as the forming of the part features with at least two dimensions in the submillimeter range [3]. **Figure 2** presents some microparts made by microforming processes.

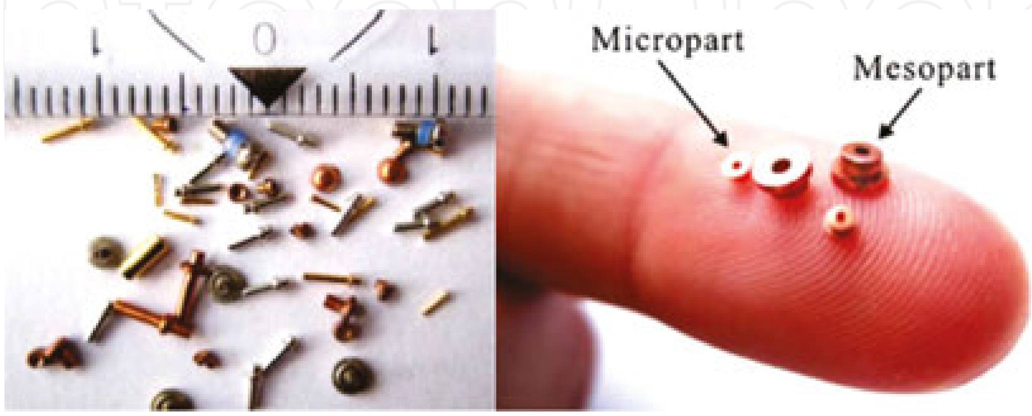

Figure 2. Mechanical microparts formed by microforming [7, 8].

Figure 3 presents all the issues which need to be considered in microforming system. There are four factors influencing the material deformation: tool-workpiece interface condition, grain size, workpiece size, and element feature size [7]. These factors further affect the efficiency of microforming system and the quality of manufactured items influencing on such a process parameters as: deformation load, forming stability (scatter of the process variables), defects of deformation, dimensional accuracy, mechanical properties, and the quality of achieved surface.

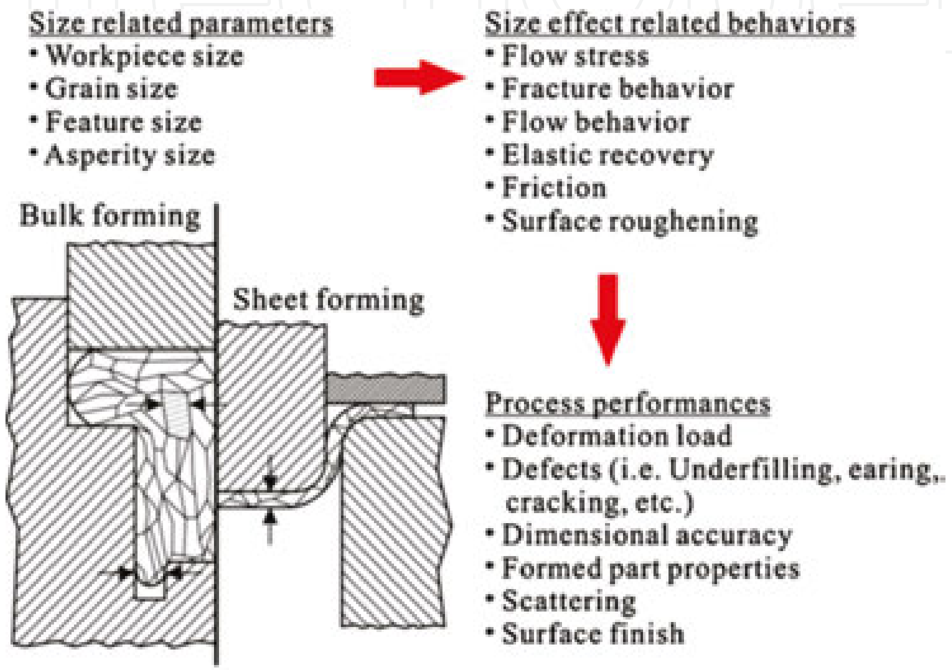

Figure 3. Issues related to size effect in microforming system [7].

The primary problem connected with microforming is the so-called "size effect" ensuing from same miniaturization. The occurrence of unpredictable changes in process parameters, while treating similar scaled workpieces, is called size effect [9]. These effects distinguish described process from conventional methods of metal forming, and significantly influence on the possibilities and limitations of this technology. Sources of size effect formation can be divided into two groups [2, 6]: physical—related to the workpiece size and the forces affecting the process; structural—induced by the microstructure of the material.

Physical sources:

- Surface-to-volume (S/V) ratio size effect—with element size decreasing, the S/V ratio increases, which makes the surface effects more crucial.
- Forces relation size effect: van der Waals forces, surface tension, and gravitation—these forces can be neglected in conventional forming processes. However, they must be taken into account in the case of microforming, because they are relatively considerable regarding the process forces and can directly affect its conditions.

Structural sources:

- Grain size to element thickness size effect—the grain size of metallic materials results from the material properties and determined by the casting condition, the thermal and mechanical treatments. It is impossible to obtain each material with each grain size, thus the grain size cannot be scaled down in parallel to the element dimension. **Figure 4** schematically shows microformability of polycrystalline and amorphous materials.

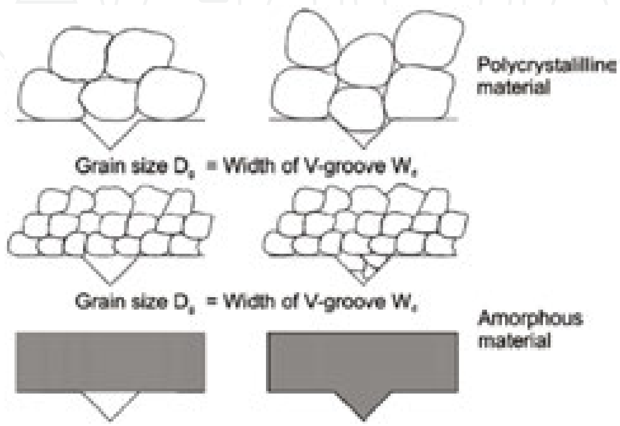

Figure 4. Microformability of polycrystalline and amorphous material [10].

In conventional metal forming operations all treated materials are considered as homogeneous. In microforming processes they are heterogeneous, because of relatively large grains size to the billet volume. As the grain size increases, the grain structure of the billet becomes to be more heterogeneous and the material shows anisotropic behavior in the submillimeter dimensional range. The anisotropic behavior of the workpiece material can directly change local deformation mechanisms as shown in **Figure 5**.

- Surface structure scalability (SSS) size effect—similarly to grain size, it is often not possible to reduce the die and billet surface roughness with the element dimension, due to that the surface structure scalability is the source of size effects. In lubrication as well as in dry conditions, SSS leads to a size-dependent friction behavior.

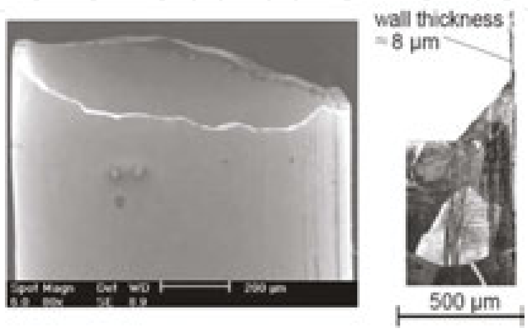

Figure 5. Backward extrusion of a billet composed of heterogeneous grain structure [3].

http://dx.doi.org/10.5772/64275

Microforming is a relatively young technology, developed in the last two decades, but more and more research centers in the world deal with it. Together with reports of experimental work results, attempts of identified numerical simulating phenomena are undertaken and presented.

2. Influence of size effects on deformation behavior in microforming processes

2.1. Flow stress

Flow stress decreases as workpiece size decreases [5, 11, 12]. Surface grains of the deformed material have lesser constraints compared to internal ones. Distribution of dislocations in surface grain boundaries is different from that of internal. The surface grains have a lower flow stress. When the plastically treated detail size is decreased to microscale and the grain size is relatively large, there are small number of grains constituting the workpiece and the volume fraction of surface grains increases significantly—surface layer model (**Figure 6**). Analogously, increase of grain size in small element reduces their number in its volume. This leads to decrease of grainy material flow stress in microscale (**Figure 7**).

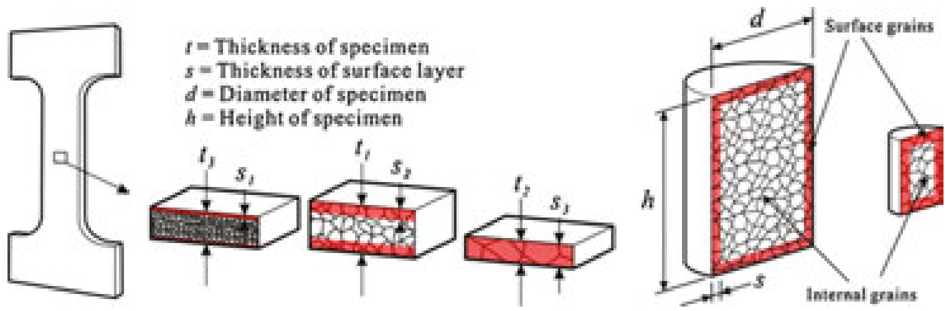

Figure 6. Change of surface grains volume fraction with decreasing of specimen size—surface layer model [13, 14].

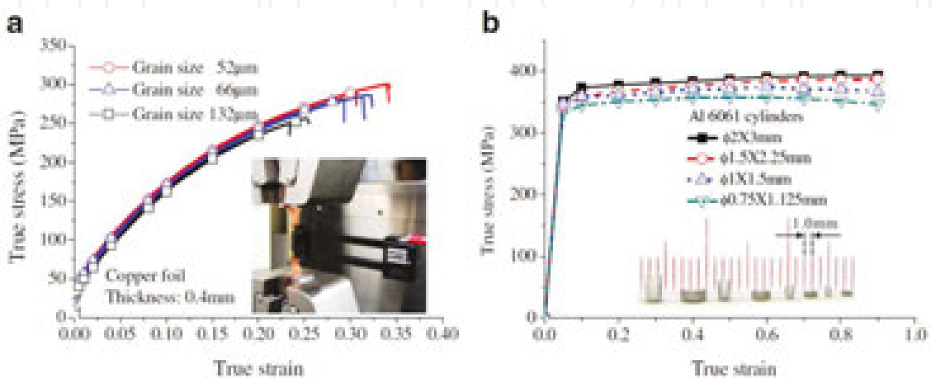

Figure 7. Grain and specimen flow stress size effects in: (a) tensile; (b) compression tests [13, 15].

2.2. Fracture

Similarly to flow stress, fracture strain decreases with the decrease of specimen size [16, 17] and the increase of grain size [12]. This phenomenon was found in tensile tests of wire and thin details. Fracture takes place through the localized shearing in the individual grain (**Figure 8**) [18–20]. The fracture strain increases also with the decrease of workpiece size in compression of bulk metal [21]. The tensile-tested material in microscale can be considered as a chain and each specimen's perpendicular section acts as a chain link (**Figure 9**). Material yields when all the grains in the section yield and the initial yielding occurs at the weakest section consisting of the soft grains [23]. The smaller the number of grains in the section, the higher the probability to find one with a significantly large fraction of soft grains decreasing the fracture strain.

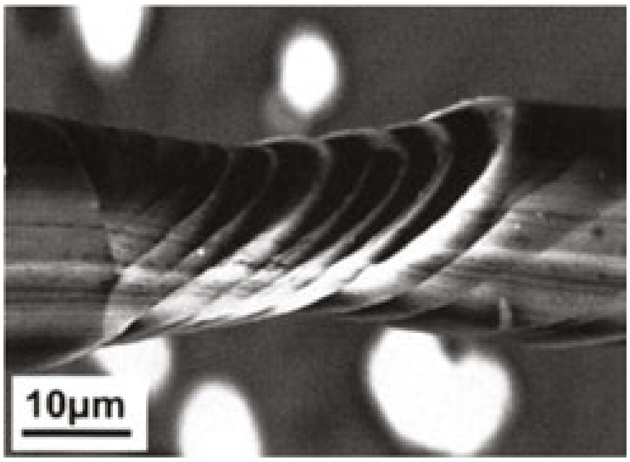

Figure 8. Scanning electron micrograph of a tensile-tested aluminum wire with a diameter of 25 μm [18].

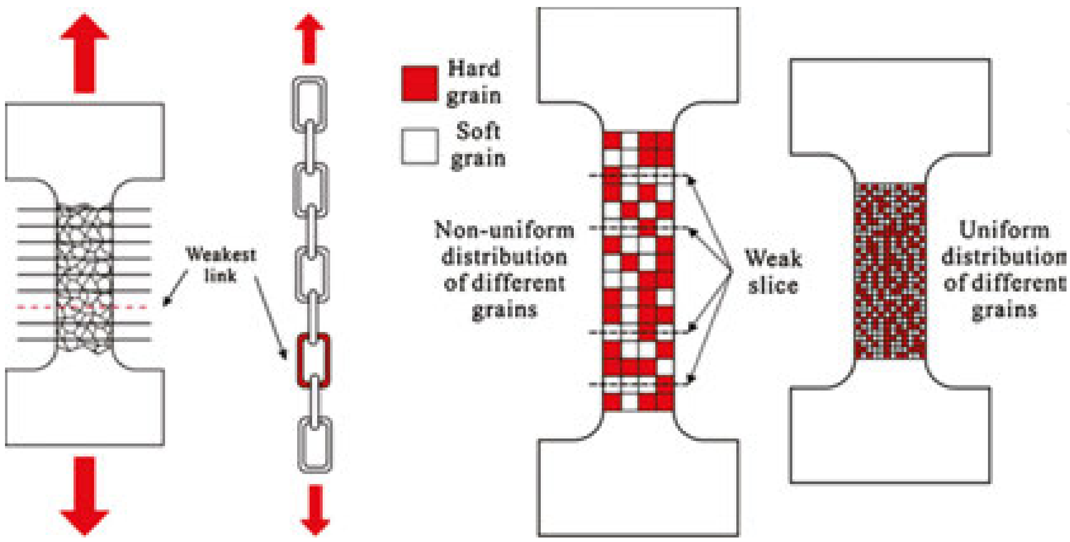

Figure 9. Schematic illustration of yielding at the weakest section of extended material [22].

http://dx.doi.org/10.5772/64275

2.3. Flow behavior

Inhomogeneous and anisotropic material behavior causes the irregular flow of formed workpiece geometry with the decrease of its size and the increase of grain size [24]. Chan et al. [12] experimentally presented decrease of flow stress, scatter of obtained data, and inhomogeneous specimen deformation with decrease of the ratio of element size to its grain size. Flow stress decrease because of grain boundary surface area to billet volume ratio gets small and the grain boundary strengthening effect is reduced. In addition, when the workpiece volume contains only a few grains (**Figure 10**), their size, shape, and orientation affect the deformation process significantly, leading to the scatter of the obtained data, for example stress-strain curves (**Figure 11**), and to the inhomogeneous billet deformation.

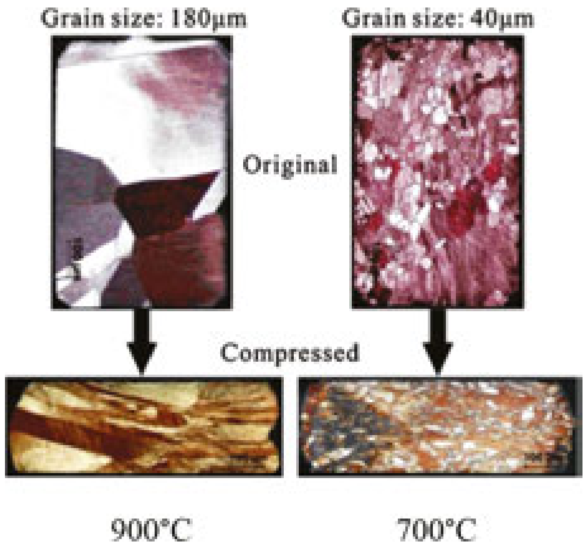

Figure 10. Microstructures of compressed specimens annealed in different temperatures [12].

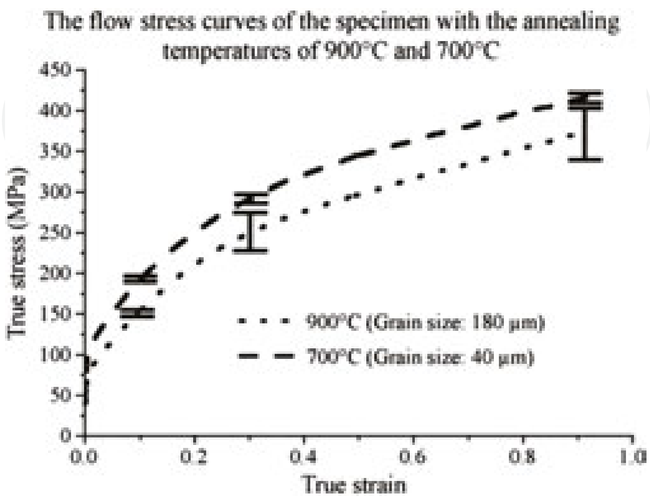

Figure 11. Flow stress curves of the billets with different grain size [12].

Flow stress size effect (**Figure 12**) and inhomogeneous deformation behavior were included in FE simulation of microcompression tests. Grain properties composite model was proposed. Grains were divided into several groups with assigned corresponding stress-strain curves. The flow stress curves of the testing samples and the scatter effect can be then estimated based on Eq. (1):

$$\sigma(\varepsilon) = \sum_{i=1}^{n} V_i \cdot \sigma_i(\varepsilon) \tag{1}$$

where n is the total number of grains in the billet, V_i is the volume fraction (area fraction in two-dimensional case) of the ith grain, and $\sigma_i(\varepsilon)$ is the flow stress of the ith grain.

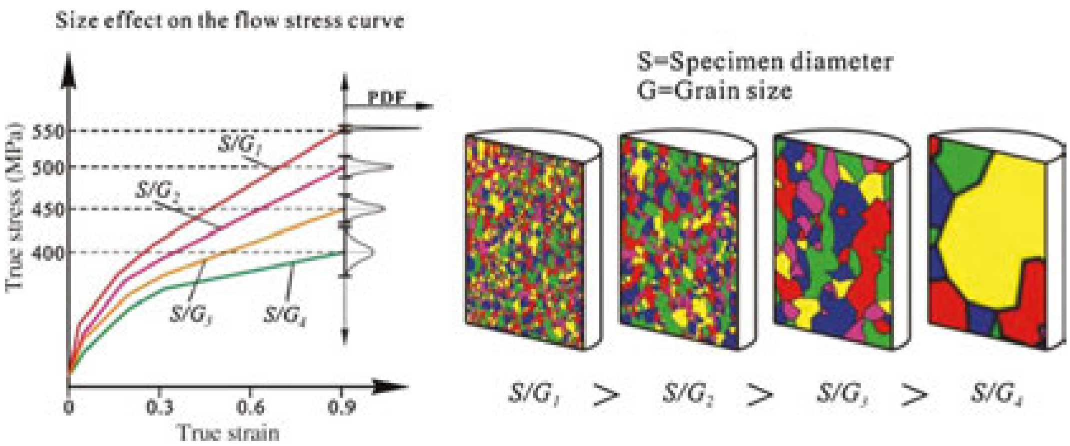

Figure 12. Illustration of flow stress size effect [12].

The volume/area fraction of each grain in the testing sample was estimated based on metallographies. The flow stress curves were then assigned to the grains randomly, as it is shown in **Figure 13**.

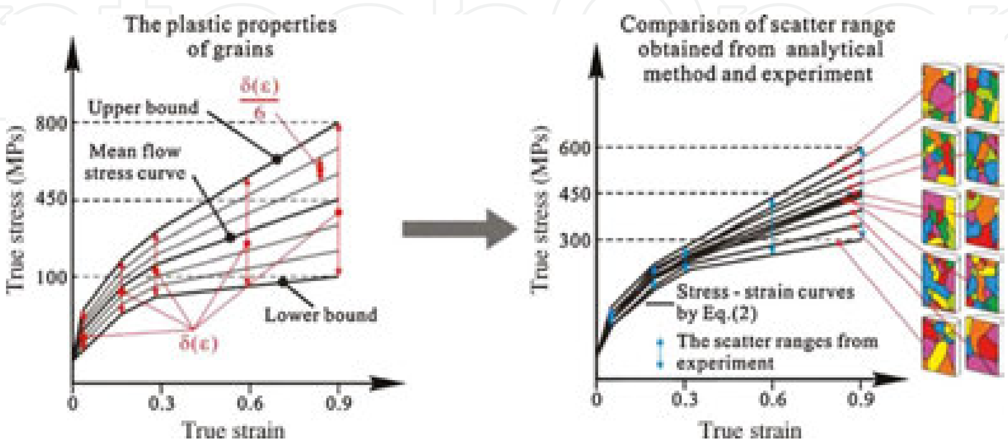

Figure 13. Spread $\sigma(\varepsilon)$ of the grains flow stress-strain curves [12].

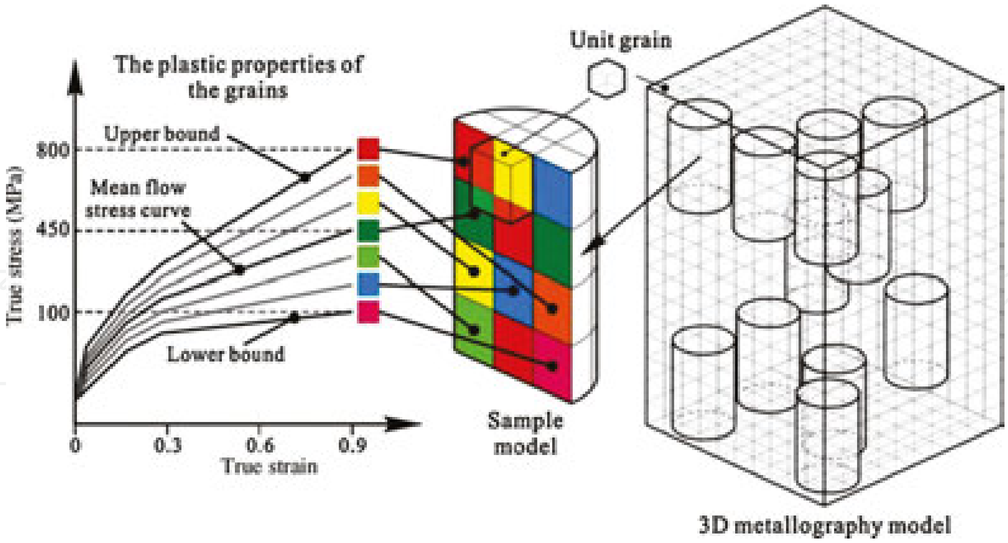

Figure 14. Schematic illustration of the 3D full-scale model with cubic grain.

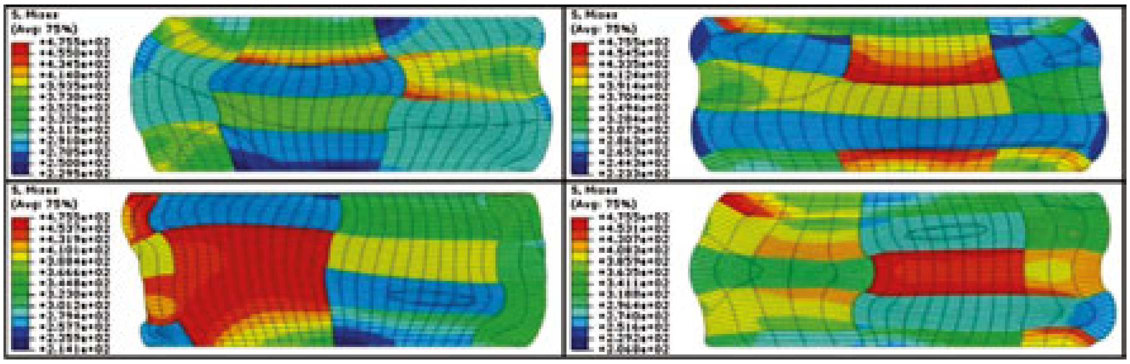

Figure 15. Stress distribution in the 3D full-scale models with surface-to-grain ratio of 2.8 [12].

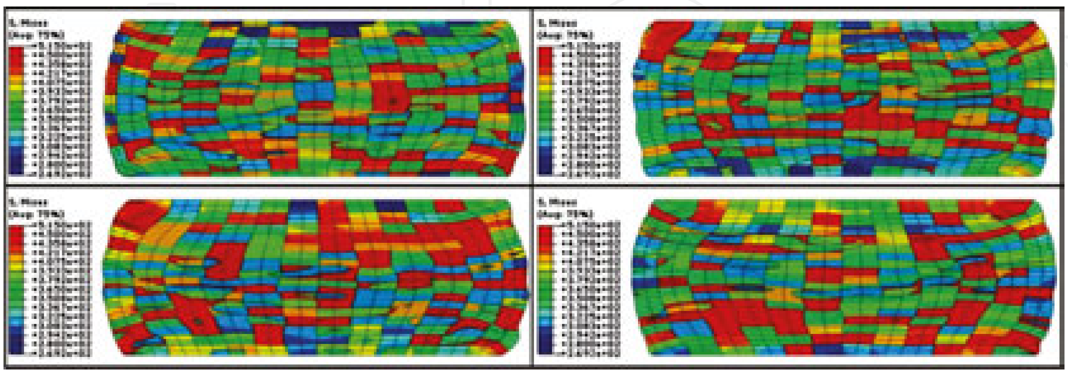

Figure 16. Stress distribution in the 3D full-scale models with surface-to-grain ratio 12.5 [12].

3D full-scale simulations using a commercial CAE system, ABACUS, were conducted with eight-node linear brick element. Grain was represented as a cube for simplification

(**Figure 14**). The grain properties identified by Eq. (1) were employed into the models. The grain interior and grain boundary were considered as a single body, while the change of grain boundary strengthening effect due to the change of surface-to-grain ratio was taken into account with varying the mean flow stress of grains. FE simulation of compression of billets consisting of individual grains results showed the inhomogeneous workpiece deformation with the decreasing ratio of specimen size to grain size (**Figures 15** and **16**). In 3D full-scale model, the asymmetry of the material deformation behavior and grain properties was taken into account. The results showed that the scatter effect of the flow stress curve increases with increasing grain size and the achieved scatter range had a good agreement with the experimental result.

Holding time (h)	0.1	0.5	2	8
Grain size (μm)	59	125	240	470
λ	7.5	3	1.6	0.85
Microstructures				

Figure 17. Microstructure of specimens and grain size, λ = specimen radius/grain size [25].

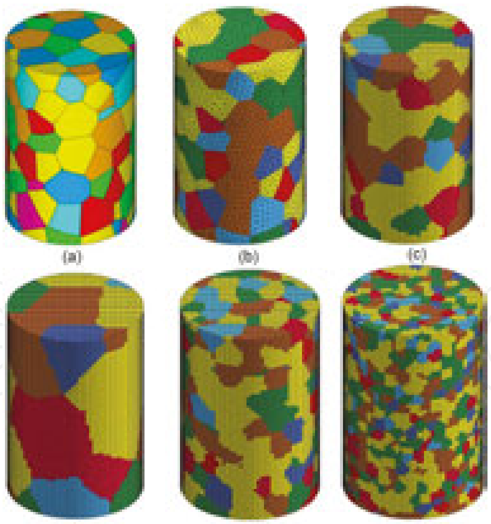

Figure 18. Aggregates of polycrystalline (a) tessellation in 140 Vornoi polyhedral; (b) freely meshed model with 140 subdomains; (c–f) Microstructure mapping on a 1313 × 60 cubic element mesh and domain with subdomain numbers 140, 26, 385, and 2520, respectively [25].

Voronoi tessellation can be adopted to describe the polycrystalline aggregate [25–27]. Lu et al. [25] proposed a mixed material model based on modified Hall-Peth relationship, surface layer model, and grained heterogeneity (e.g., grain size, shape, and deformability). Pure copper compression experiment was performed (**Figure 17**). Generated virtual microstructures which can be implemented in the commercial FE code are presented in **Figure 18**.

The deformed part can be represented by a space tessellation into 3D Voronoi diagram which describes grain boundary [25]. Voronoi diagram is defined as n distinct regions, V_i based on an open set Ω, and n different seeds z_i ($i = 0, 1,\ldots, n - 1$) such as:

$$V_i = \left\{ w \in \Omega \quad d\left(w, z_j\right) j = 0,1,\ldots, j \neq i \right\} \tag{2}$$

where d is the function of distance. Voronoi polyhedra are the influence zones of these grains that are their mass center.

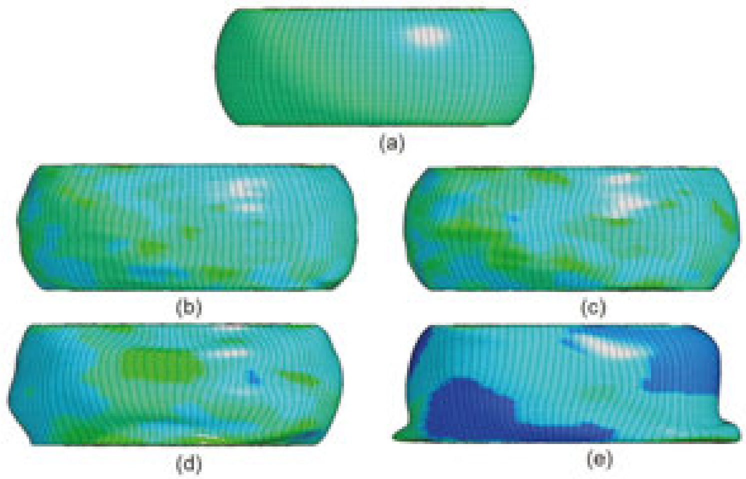

Figure 19. Profile of specimens after compression, (a) homogenous model with $\lambda = 1.6$, (b) $\lambda = 7.5$, (c) $\lambda = 3$, (d) $\lambda = 1.6$, (e) $\lambda = 0.85$ [25].

A 3D domain is decomposed into a certain number of subdomains. Then, the seeds are spread into these subdomains. Assuming the center of a cube is (x, y, z), the seed will lie $\lambda\delta a/2$ away from the central point. The coordinate of the seed position should be ($x + \lambda\delta a/2$, $y + \lambda\delta a/2$, $z + \lambda\delta a/2$). δ is the maximum distance between the seed and the cubic center, and λ is a random number between −1 and 1. Both δ and λ are the so-called shape factors which will determine the shapes of the Voronoi cells. A critical distance d between different seeds is defined to prevent each seed from being too close to another. After that, 3D Voronoi polyhedra can be generated by taking these seeds as the generating points [25].

Obtained from nanoindentation hardness of grains was used to identify the deformability of individual grain inside the billet. Applying developed material model, the microcompression test of pure copper was numerically simulated (**Figure 19**) using commercial the FEM software ANSYS/LS-DYNA. Numerical analyses results show that the scatter of deformation behavior becomes significant with decreasing factor λ, where λ is the specimen radius/grain size.

2.4. Elastic recovery

Springback increases with decreasing ratio of workpiece thickness to grain size [15, 28]. Liu et al. [15] used the pure copper sheet foils with the thickness from 0.1 to 0.6 mm as the testing material for tensile test and microbending (**Figure 20**). It was founded that the springback angle increases with the decreasing metal element thickness. This is consistent with the conventional bending knowledge specific for macroscale bending. Increase in the scatter of springback angle with decreasing sheet thickness was also found. It was concluded that the main reason for that is elastic anisotropy of surface grain due to grain orientation difference.

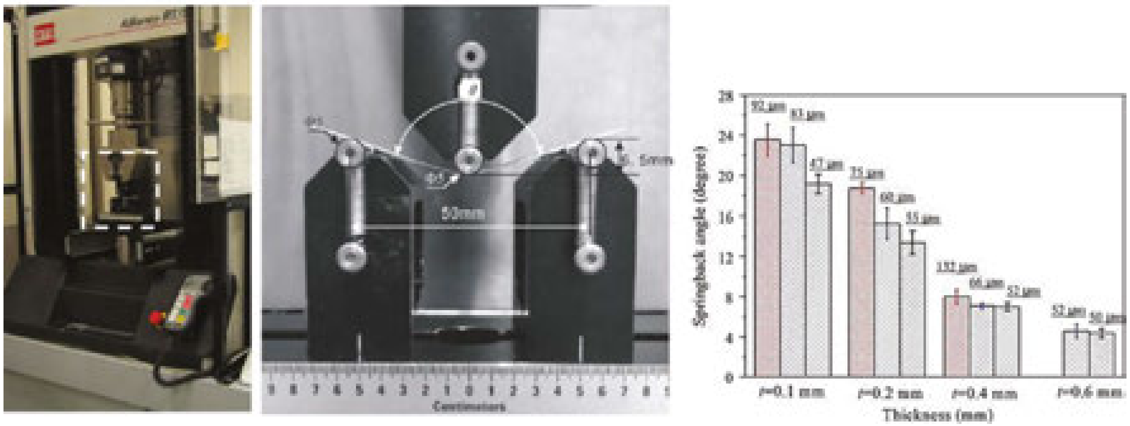

Figure 20. Left: Three-point bending test device and tooling; Right: Influence of grain size on springback angle [15].

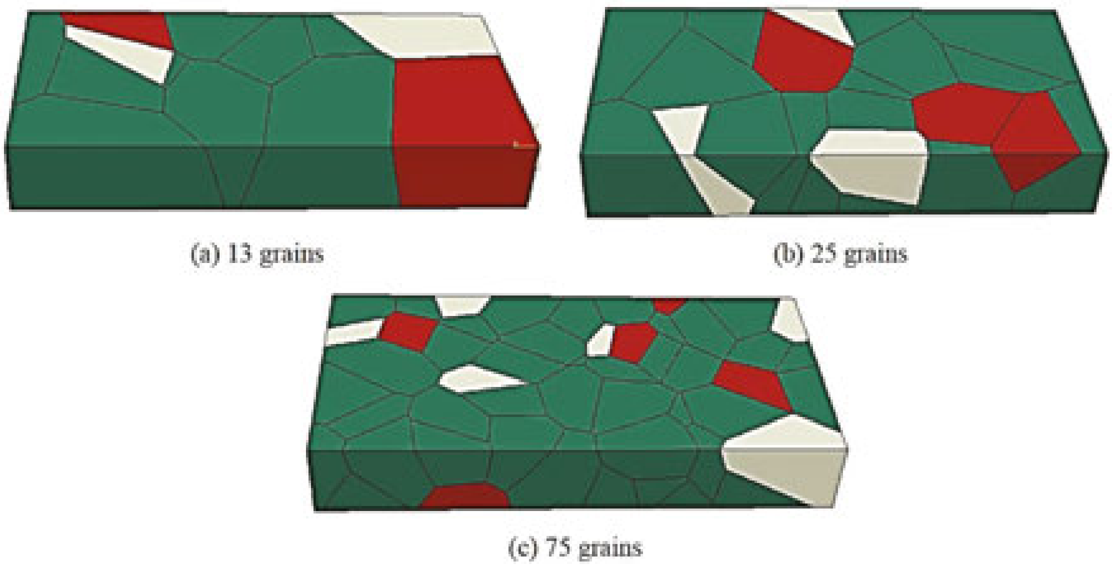

Figure 21. Grained heterogeneity in workpiece with: (a) 13 grains; (b) 25 grains; and (c) 75 grains [29].

Fang et al. [29] conducted numerical simulation to investigate the size effect of the springback, which occurs after the micro-V-bending in terms of Voronoi tessellation. A finite element

http://dx.doi.org/10.5772/64275

model of the micro-V-bending has been designed by using the ABAQUS/Standard commercial software. The workpiece grain sizes of 98, 152, and 201 μm have been adopted in the FE model (**Figure 21**) to recognize the relationship between the size effect and springback angle during the V-bending process. Voronoi tessellation can imitate the microstructure of materials, and represents grained heterogeneity graphically in FE models. Grains were divided into three groups with assigned corresponding stress-strain curves (**Figure 22**). Simulation results display the inhomogeneous deformation behavior during micro-V-bending process and also show that springback effect increases with grain size (**Figure 23**).

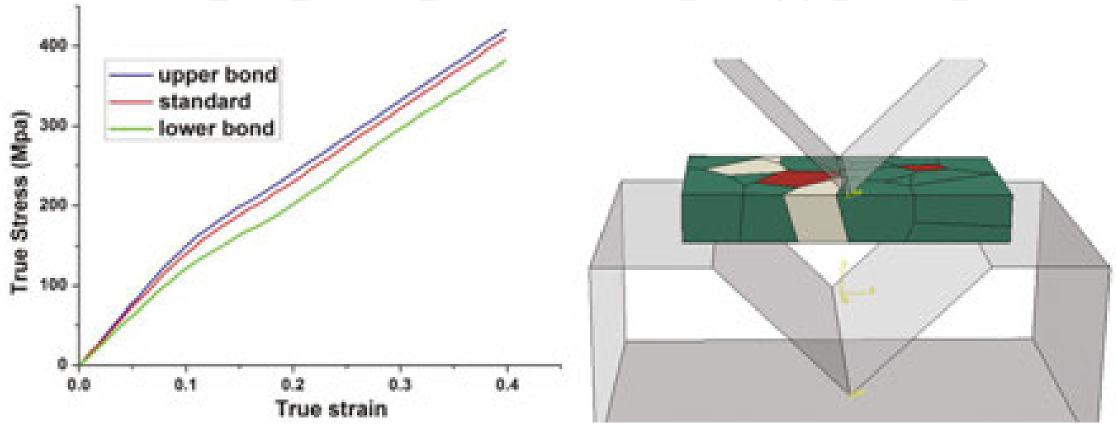

Figure 22. Left: Flow stress curves of the grains in workpiece with grain size 152 μm; Right: Micro-V-bending FE model with workpiece grain size 152 μm [29].

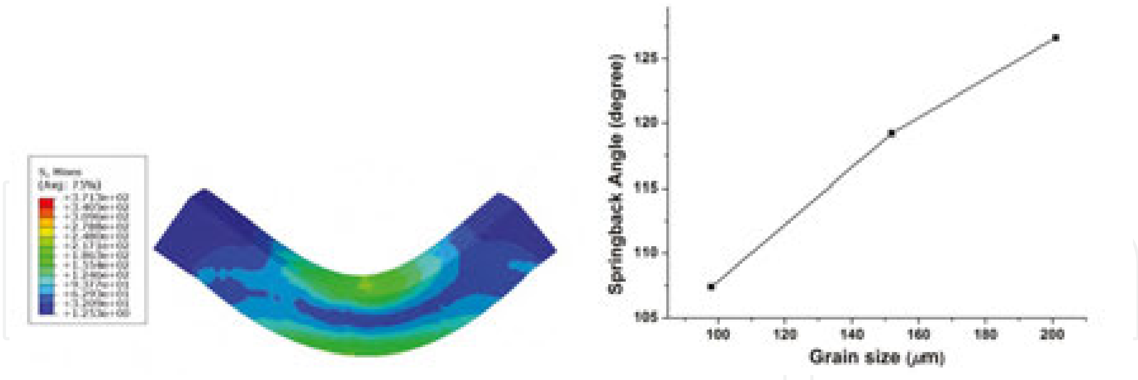

Figure 23. Left: Micro-V-bending result after unloading; Right: Springback angle with different grain size [29].

2.5. Frictional behavior

2.5.1. Open and closed lubricant pockets (CLPs)

Changes of interfacial friction with the decrease of element size in microforming process can be estimated based on the size-scaled ring compression test [5] and double-cup extrusion

(DCE) [30]. The friction is recognized based on the comparison between the geometry of the deformed sample and the finite element simulations results. Change of friction factor with decreasing workpiece size in the DCE process in lubricated conditions is presented in **Figure 24**. It can be seen that the friction increases with the scaled down workpiece size [30].

To recognize the frictional behavior in microforming, the asperity deformation process needs to be taken into account. Surface topography evolution process is shown in **Figure 25**. Before the tool touches the workpiece surface, there is a layer of lubricant on the whole contact surface (**Figure 25a**). When the tool presses the workpiece surface, some lubricant is trapped in the roughness valleys, which results in the formation of the so-called closed lubricant pockets (**Figure 25b**). In the CLPs, a hydrostatic pressure is thus generated and part of the deformation load is shared by the lubricant. Under this condition, material slides along the tooling surface with low friction. At the workpiece edges the lubricant is squeezed out from the roughness valleys and the so-called open lubricant pockets (OLPs) are then created. At the OLPs, the flattened asperities support deformation load and they become to be the real contact areas (RCAs), which increases the interfacial friction (**Figure 25c**). Open and closed pockets model application in FE simulation is presented in **Figure 26** [32]. Presence of CLP and OLP results in the nonuniform deformation of material asperities surface affects the surface properties of the formed microelement.

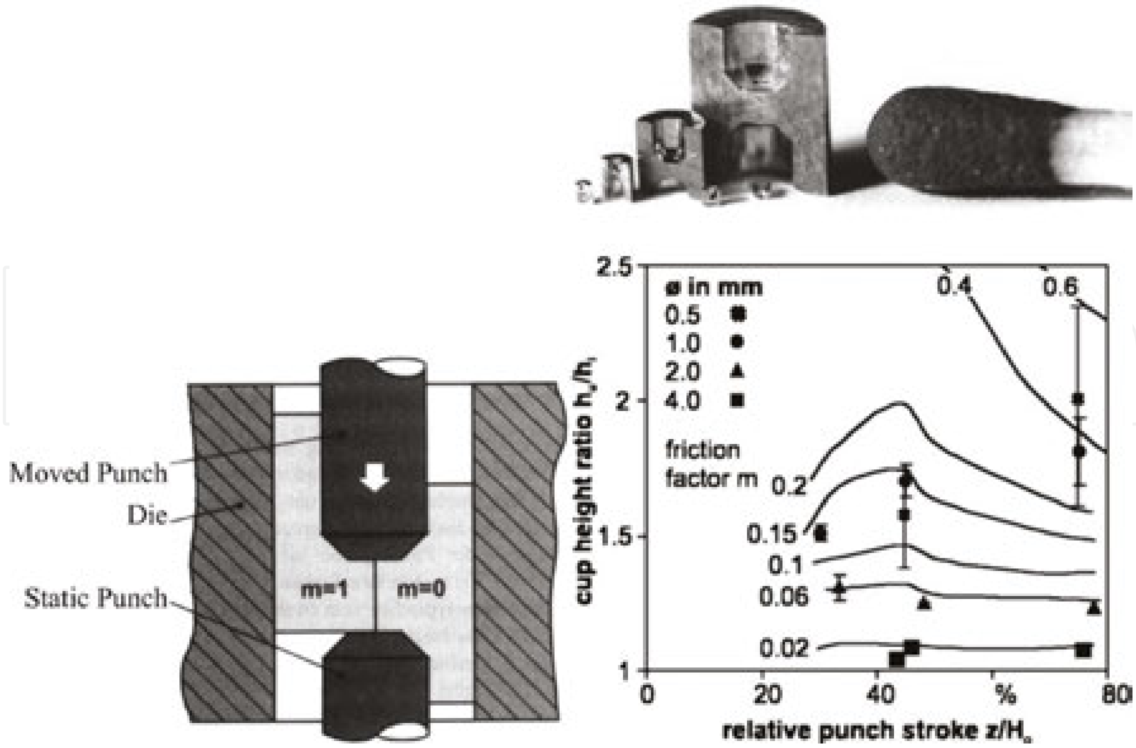

Figure 24. The formed geometries in different size-scaled achieved in double-cup extrusion tests [31].

http://dx.doi.org/10.5772/64275

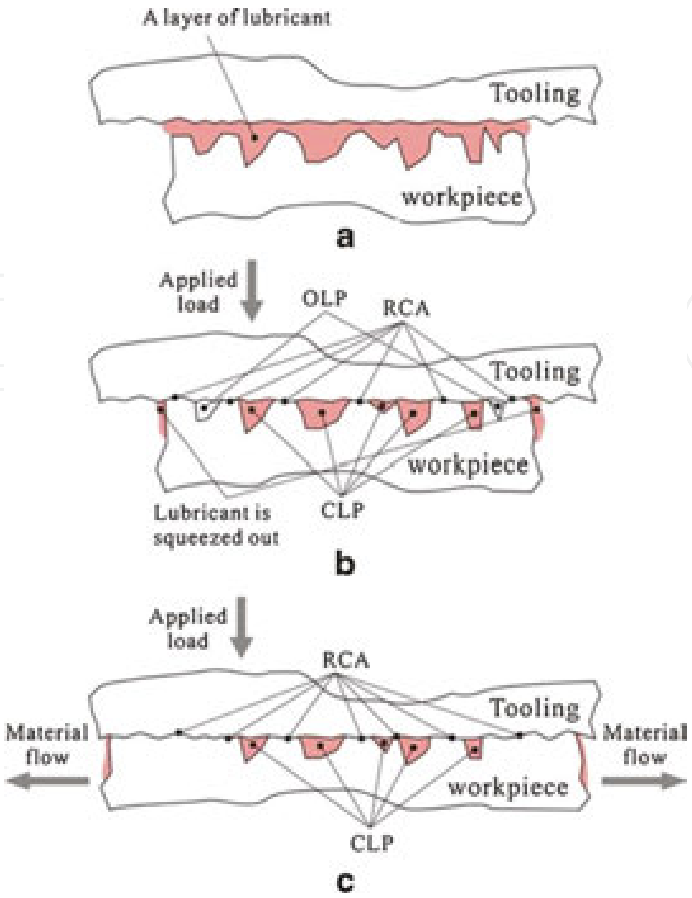

Figure 25. The evolution of workpiece surface asperities in deformation process [32].

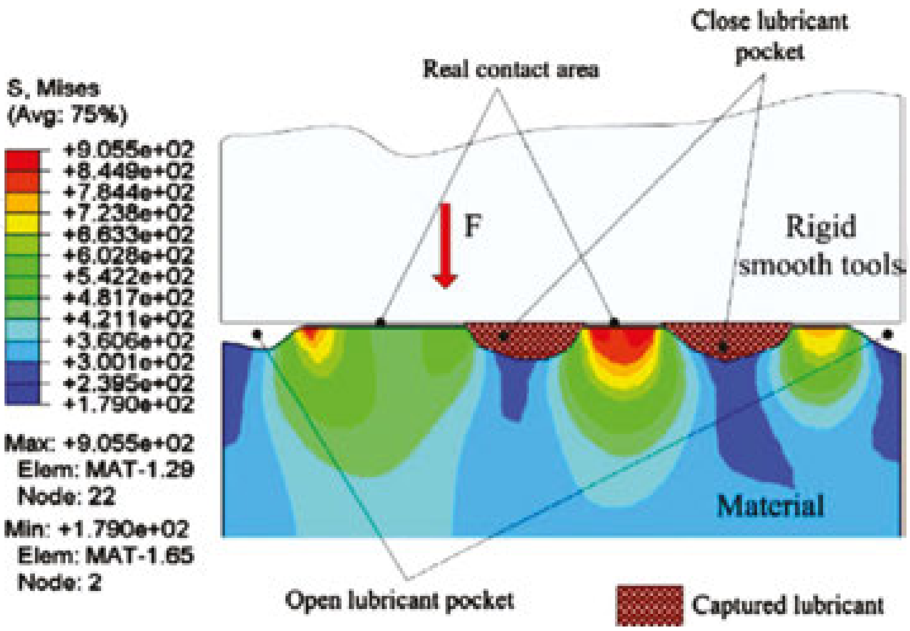

Figure 26. 2D sketch of OLPs, RCAs, and CLPs [32].

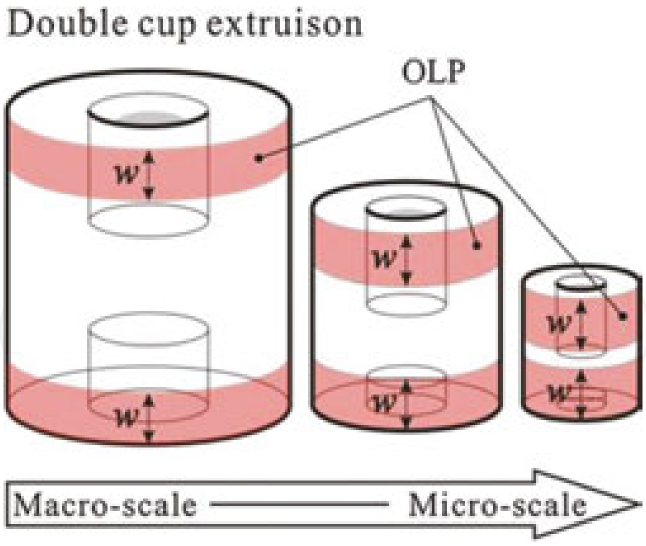

Figure 27. The increase of OLP fraction with the decrease of workpiece size [7].

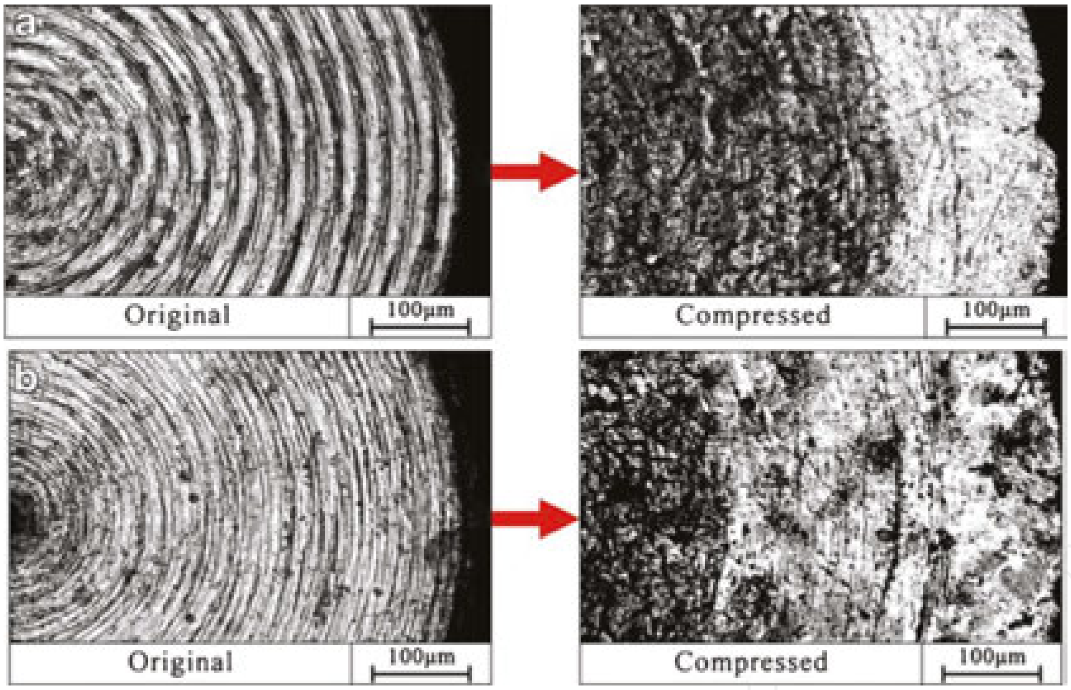

Figure 28. End surface topographies of the specimens (Ø1 × 1.5 mm) with the asperity size of: (a) 25 μm; and (b) 10 μm [32].

Increase of friction with miniaturization is related to the increase of OLP fraction (**Figure 27**). The influence of different sizes of asperity on the change of the compressed surface topography is shown in **Figure 28**. The thickness of OLP rim decreases with the increase of asperity size. This reveals that the efficiency of lubricant in load supporting is higher in the surface with large asperities. More lubricant can be then trapped in the roughness valleys, resulting in the increase of the CLP area fraction.

2.5.2. *Friction in forward and backward cup extrusion*

Material tends to flow backwards (higher cup) with the decrease of the workpiece size when the fine-grained material is used [31]. Coarse grain size (**Figure 29**, case 0.5 mm) is larger than the cup wall thickness, which makes the material flow forward easily (longer shaft). Deformation behavior of fine- and coarse-grained samples in microdouble-cup extrusion is showed in **Figure 30**.

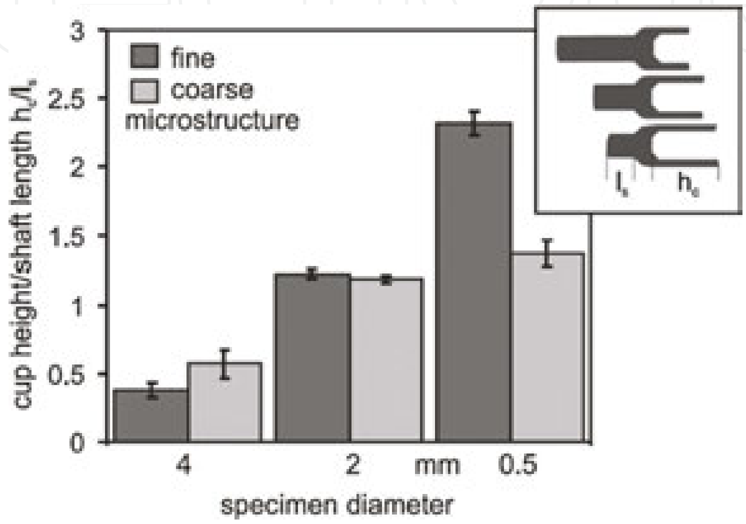

Figure 29. The experimental results of the combined forward rod—backward cup extrusion [31].

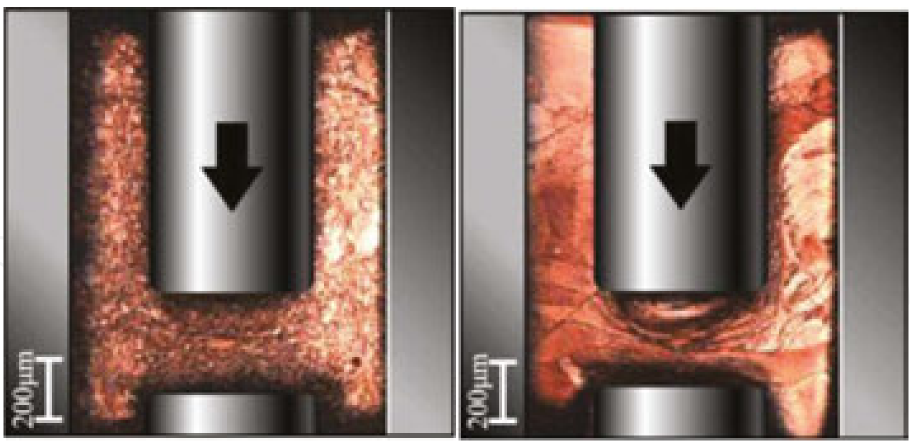

Figure 30. Microstructures of the microformed parts in microdouble-cup extrusion with different grain sizes. (a) 20 and (b) 150 μm [33].

2.5.3. *Surface roughening*

The ratio of tool asperity size to the formed element size increases with decrease of workpiece size and the increase of grain size [22, 34, 35]. Die workpiece interface effects become significant in microforming. Geiger et al. [31] has shown that the use of the traditional friction coefficient or friction factor can lead to erroneous results in microscale. Some of the researchers have taken into account the impact of degree of a tool roughness on the material deformation process in numerical analysis. Challen et al. [36] presented the friction model for rough contact of plastic material with a rigid tool. Model is based on a simplified geometry of the tool surface, whose actual profile reflects a triangular wave (**Figure 31**). The surface roughness used in the model is the average of the asperities parameters measured in the experiment.

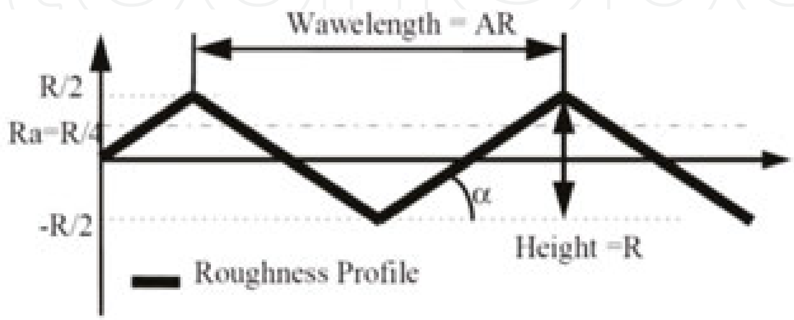

Figure 31. Triangular wave surface roughness model [36].

In that way, using a commercial FE system DEFORM, geometry of the tool surface was modeled in experimentally verified simulations of the forward microextrusion processes [37, 38] (**Figure 32**), where a significant influence of container roughness on the material flow was shown.

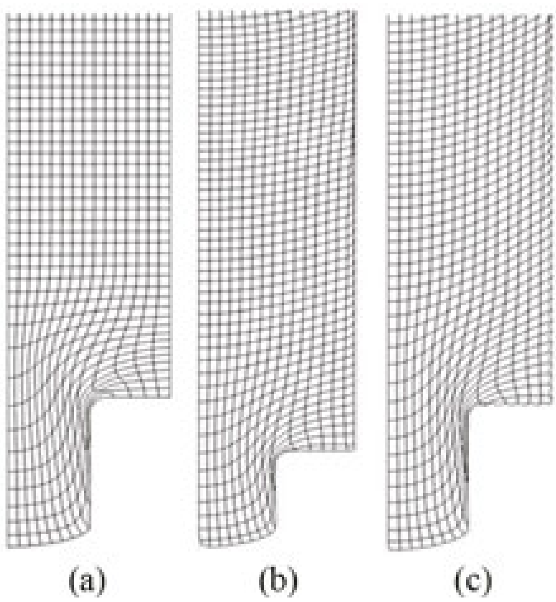

Figure 32. Flow nets of microextruded metal rods with a tool surface characterized by: (a) constant friction factor; (b) and (c) rigid triangular waves [39].

Vidal-Sallé et al. [40, 41] modeled die roughness in the form of a rigid triangular wave and the wave of interconnected arcs—model machined by turning surfaces in FE simulations of cylinder compression (**Figure 33**).

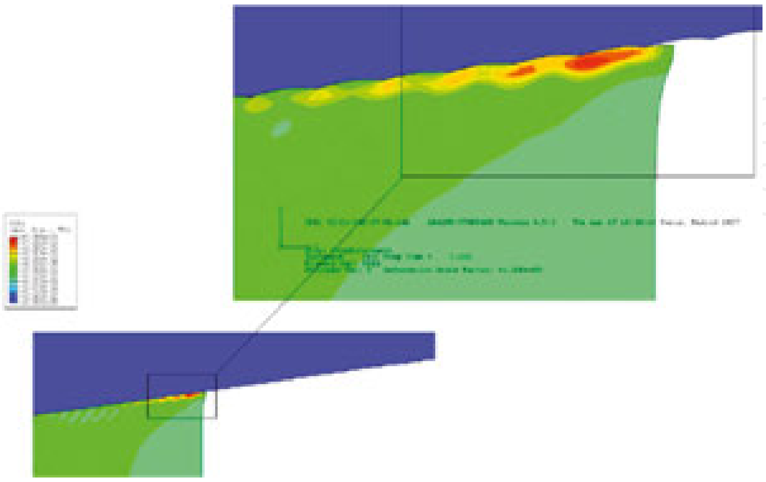

Figure 33. Plastic strain distribution in the compressed billet for perfect sliping [41].

Jeon et al. [42, 43] modeled die surfaces in the form of rigid sinusoidal curve in numerical simulation of the ring compression (**Figure 34**) as opposed to the use of the traditional empirical friction coefficient or factor. This finite-element-based model has been validated experimentally in terms of loads and metal flow using the ring test and actual surface measurements. The curve was referenced to the parameter *Ra* and the friction factor was determined as $m = f(a,t)$.

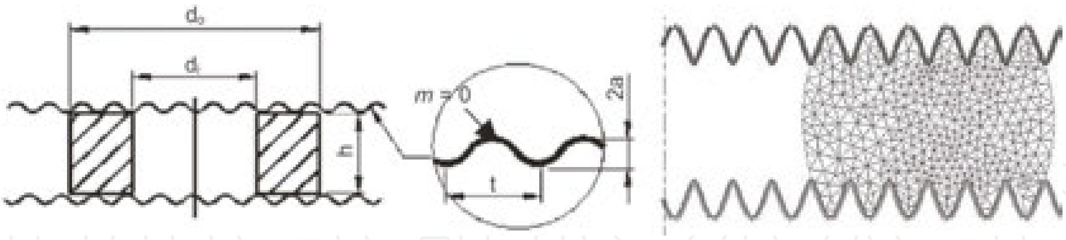

Figure 34. Tool surface geometric model with using an elliptical profile [42].

2.6. Repeatability

The scatter of the measured material properties (**Figure 35**) (e.g., flow stress, material deformation behavior) increases with the increase of grain size and the decrease of the workpiece size. This phenomenon is the resulted of different properties of individual grains and their less number in the workpiece volume [11, 44]. The deformation behavior of a single grain has an anisotropic nature. When the specimen size decreases and the grain size stays constant, there will be a small number of grains in the specimen volume and so the number of microstructural features decreases. The uniform distribution of different grains no longer exists. Each grain with each property plays a significant role to the overall material deformation behavior. Different crystallographic orientations, different shapes, and sizes of neighboring grains lead to inhomogeneous deformation, which result in the scatter of achieved material properties.

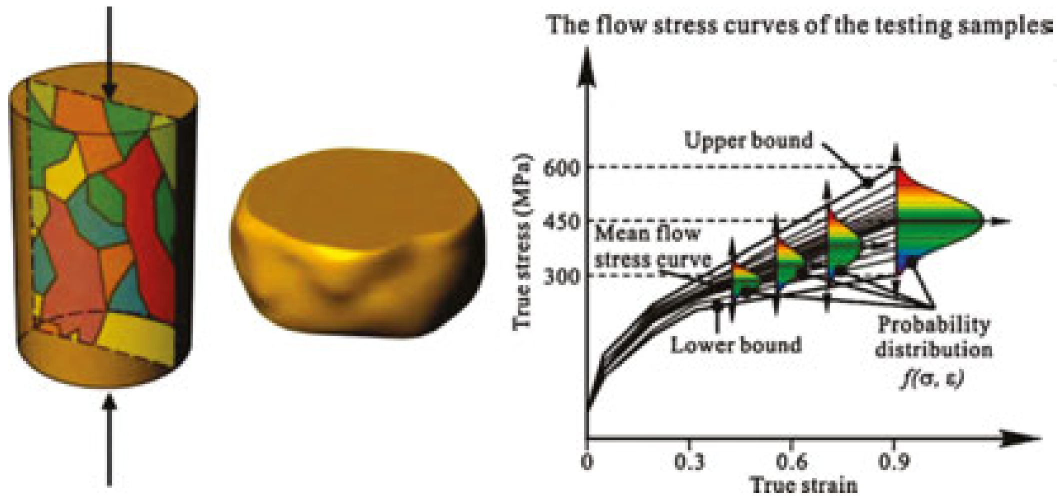

Figure 35. Schematic illustration of the modeling of the scatter effect with a normal distribution function [12].

2.7. Mechanical property of the formed billet

The hardness distribution of the formed billet becomes to be no uniform in microforming (**Figure 36**) when the grain size is coarse [45, 46]. More even material flow and hardness distribution can be achieved using the ultrafine-grained material. This implies the potential applications of the ultrafine-grained materials in metal microforming processes.

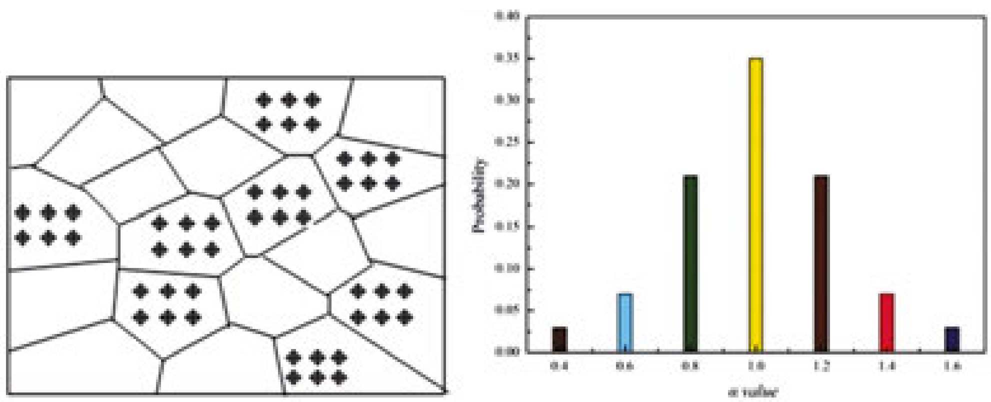

Figure 36. Left: Illustration of nanoindentation; Right: statistical distribution of α-value, α—ratio of the hardness at each class to the average hardness [25].

Billet formability increases with the decrease of workpiece size for a constant grain size [21]. It needs a larger strain to initiate cracking in microforming (**Figure 37**). Common assumption

http://dx.doi.org/10.5772/64275

is that the damage energy to initiate fracturing is the same in macro- and microscale. The flow stress decreases with the billet size, so the larger deformation is needed to obtain the critical damage energy in microforming.

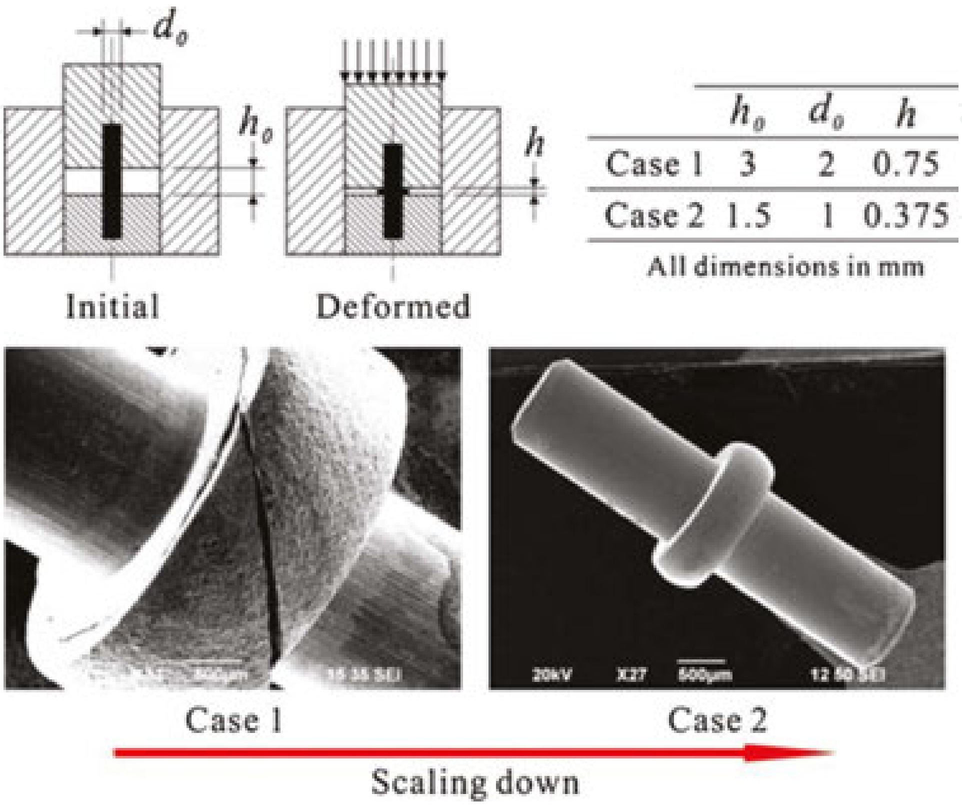

	h_0	d_0	h
Case 1	3	2	0.75
Case 2	1.5	1	0.375

Figure 37. Different size-scaled central headed parts [21].

2.8. Summary

Microforming is considered as an economically competitive process for production of metallic microcomponents. The scaling down of a forming system from macro to micro leads to the occurrence of size effect. This phenomenon differs microforming from forming in macroscale and do not allow applying conventional knowledge. The anisotropic properties of each grain, the random nature of grain distribution, and orientation as well as tool surface roughness become significant. This leads to the inhomogeneous deformation and the scatter of the achieved flow stress. Experimentally recognized size effects, such as flow stress size effect, deformation behavior size effect, or interfacial friction size effect are numerically modeled, giving the ability to more accurately identify their mechanics and to predict the results of the microforming process.

For the microforming process simulations, commercial FE systems such as DEFORM, QFORM, ABACUS, or ANSYS/LS-DYNA are used. Nonlinear code ADINA (developed by KJ Bathe and his team at MIT Mechanical Engineering) may be also recommended to solve some of the complex multiphysical micromechanics phenomena associated with metal forming. Grain structures are modeled based on metallographies or using Voronoi tessellation and the tool surface roughness using rigid waves. Ortiz atomistic models of material behavior based on atomistic energy laws may be an alternative way to resolve the mechanics of microforming of metals.

Although the polycrystalline material deformation behaviors have been extensively studied and adopted in numerical simulations, the size effects physics is not yet thoroughly understood. The influence of size effect on deformation mechanics in microforming processes is still a challenging issue to be investigated.

Acknowledgements

This chapter has been carried out in the framework of the S/WM/1/2015 statutory work and financed from the Ministry of Science and Higher Education funds.

Author details

Krzysztof Mogielnicki*

Address all correspondence to: k.mogielnicki@pb.edu.pl

Bialystok University of Technology, Bialystok, Poland

References

[1] Teyfouri A, Ahmadi M, Sorooshian S. Mint: A review on micro formings. Modern Applied Science 9(9). 2015;230.

[2] Vollertsen F, Schulze Niehoff H, Hu, Z. Mint: State of the art in micro forming. International Journal of Machine Tools and Manufacture 46(11). 2006;1172–1179.

[3] Engel U, Eckstein R. Mint: Microforming – from basic research to its realization. Journal of Materials Processing Technology 125. 2002;35–44.

[4] Vollertsen F, Biermann D, Hansen HN, Jawahir IS, Kuzman K. Mint: Size effects in manufacturing of metallic components. CIRP Annals – Manufacturing Technology 58(2). 2009;566–587.

[5] Messner A, Engel U, Kals R, Vollertsen F. Mint: Size effect in the FE-simulation of microforming processes. Journal of Materials Processing Technology 45(1–4). 1994;371–376.

[6] Vollertsen F, Hu Z, Niehoff HS, Theiler C. Mint: State of the art in micro forming and investigations into micro deep drawing. Journal of Materials Processing Technology 151(1–3). 2004;70–79.

[7] Fu MW, Chan WL. Mint: A review on the state-of-the-art microforming technologies. The International Journal of Advanced Manufacturing Technology 67(9–12). 2013; 2411–2437.

[8] Chan WL, Fu MW. Mint: Meso-scaled progressive forming of bulk cylindrical and flanged parts using sheet metal. Materials & Design 43. 2013;249–257.

[9] Kahnis P. Analyse von Größeneinflüssen beieiner Herabskalierung des Fräsprozesses in den Mikrobereich. [Dissertation] Technische Universität Dortmund, Vulkan Verlag Essen; 2008.

[10] Saotome Y, Zhang T, Inoue A. Mint: Microforming of MEMS parts with amorphous alloys. In MRS Proceedings, Vol. 554. Cambridge University Press; 1998. 385 p.

[11] Diehl A, Engel U, Geiger M. Mint: Influence of microstructure on the mechanical properties and the forming behaviour of very thin metal foils. The International Journal of Advanced Manufacturing Technology 47(1–4). 2010;53–61.

[12] Chan WL, Fu MW, Lu J, Liu JG. Mint: Modeling of grain size effect on micro deformation behavior in micro-forming of pure copper. Materials Science and Engineering A: Struct 527(24–25). 2010;6638–6648.

[13] Chan WL, Fu MW, Lu J. Mint: The size effect on micro deformation behaviour in micro-scale plastic deformation. Materials & Design 32(1). 2011;198–206.

[14] Chan WL, Fu MW. Mint: Experimental studies and numerical modeling of the specimen and grain size effects on the flow stress of sheet metal in microforming. Materials Science and Engineering A: Struct 528(25–26). 2011;7674–7683.

[15] Liu JG, Fu MW, Lu J, Chan WL. Mint: Influence of size effect on the springback of sheet metal foils in micro-bending. Computational Materials Science 50(9). 2011;2604–2614.

[16] Simons G, Weippert C, Dual J, Villain J. Mint: Size effects in tensile testing of thin cold rolled and annealed Cu foils. Materials Science and Engineering A: Struct 416(1–2). 2006;290–299.

[17] Weiss B, Groger V, Khatibi G, Kotas A, Zimprich P, Stickler R, Zagar B. Mint: Characterization of mechanical and thermal properties of thin Cu foils and wires. Sensors and Actuators A: Physical 99(1–2). 2002;172–182.

[18] Khatibi G, Mingler B, Schafler E, Stickler R, Weiss B. Mint: Microcharacterization of thin copper and aluminium bond wires. BHM Berg- und Hüttenmännische Monatshefte 150(5). 2005;176–180.

[19] Khatibi G, Betzwar-Kotas A, Groger V, Weiss BA. Mint: Study of the mechanical and fatigue properties of metallic microwires. Fatigue and Fracture of Engineering Materials and Structures 28(8). 2005;723–733.

[20] Fu MW, Chan WL. Mint: Geometry and grain size effects on the fracture behavior of sheet metal in micro-scale plastic deformation. Materials & Design 32(10). 2011;4738–4746.

[21] Ran JQ, Fu MW, Chan WL. Mint: The influence of size effect on the ductile fracture in micro-scaled plastic deformation. International Journal of Plasticity 41. 2013;65–81.

[22] Chan WL, Fu MW. Mint: Experimental and simulation based study on micro-scaled sheet metal deformation behavior in microembossing process. Materials Science and Engineering A: Struct 556. 2012;60–67.

[23] Henning M, Vehoff H. Mint: Statistical size effects based on grain size and texture in thin sheets. Materials Science and Engineering A: Struct 452. 2007;602–613.

[24] Eichenhueller B, Egerer E, Engel U. Mint: Microforming at elevated temperature—forming and material behaviour. International Journal of Advanced Manufacturing Technology 33(1–2). 2007;119–124.

[25] Lu HN, Wei DB, Jiang ZY, Liu XH, Manabe K.. Mint: Modelling of size effects in microforming process with consideration of grained heterogeneity. Computational Materials Science 77. 2013;44–52.

[26] Cao J, Zhuang W, Wan S, Ho KC, Zhang N, Lin J, Dean TA. Mint: An integrated crystal plasticity FE system for microforming simulation. Journal of Multiscale Modelling 1(01). 2009;107–124.

[27] Fang Z, Jiang ZY, Wei DB. Mint: Modeling of grained heterogeneity with Voronoi tessellation in microforming process. Applied Mechanics and Materials 553. 2014;66–70.

[28] Gau JT, Principe C, Yu M. Mint: Springback behavior of brass in micro sheet forming. Journal of Materials Processing Technology 191(1–3). 2007;7–10.

[29] Fang Z, Lu H, Wei D, Jiang Z, Zhao X, Zhang X, Wu D. Mint: Numerical study on spring back with size effect in micro V-bending. Procedia Engineering 81. 2014;1011–1016.

[30] Engel U. . Mint: Tribology in microforming. Wear 260(3). 2006;265–273.

[31] Geiger M, Kleiner M, Eckstein R, Tiesler N, Engel U. Mint: Microforming. CIRP Annals – Manufacturing Technology 50(2). 2001;445–462.

[32] Deng JH, Fu MW, Chan WL. Mint: Size effect on material surface deformation behavior in micro-forming process. Materials Science and Engineering A: Struct 528(13–14). 2011;4799–4806.

[33] Chan WL, Fu MW, Yang B. Mint: Study of size effect in microextrusion process of pure copper. Materials and Design 32(7). 2011;3772–3782.

[34] Chan WL, Fu MW, Yang B. Mint: Experimental studies of the size effect affected microscale plastic deformation in micro upsetting process. Materials Science and Engineering A: Struct 534. 2012;374–383.

[35] Chan WL, Fu MW. Mint: Experimental studies of plastic deformation behaviors in microheading process. Journal of Materials Processing Technology 212(7). 2012;1501–1512.

[36] Challen JM, Oxley PLB. Mint: An explanation of the different regimes of friction and wear using asperity deformation models. Wear 53. 1979;229–243.

[37] Piwnik J, Mogielnicki K. Mint: The friction influence on stress in micro extrusion. Archives of Foundry Engineering 10. 2010;451–454.

[38] Piwnik J, Mogielnicki K. Mint: Experimental and FE analysis of aluminium alloy plastic flow in the forward micro-extrusion processes. Archives of Metallurgy and Materials 59(2). 2014;521–525.

[39] Piwnik J, Mogielnicki K. Mint: Deformations in micro extrusion of metals. Archives of Foundry Engineering (3). 2010;87–90.

[40] Vidal-Sallé E, Maisonnette-Masson S, Boyer JC. Mint: About the validity of the plastic wave model for an actual roughness of axisymmetric tooling in bulk forming. International Journal of Material Forming 2. 2009;217–220.

[41] Vidal-Sallé E, Boutabba S, Cui Y, Boyer JC. Mint: An improved «plastic wave» friction model for rough contact in axisymmetric modeling of bulk forming processes. International Journal of Material Forming 1(1). 2008;1263–1266.

[42] Jeon HJ, Bramley AN. Mint: A friction model for microforming. The International Journal of Advanced Manufacturing Technology 33. 2007;125–129.

[43] Becker P, Jeon H J, Chang CC, Bramley AN. . Mint: A geometric approach to modelling friction in metal forming. CIRP Annals-Manufacturing Technology 52(1). 2003;209–212.

[44] Raulea LV, Goijaerts AM, Govaert LE, Baaijens FPT. Mint: Size effects in the processing of thin metal sheets. Journal of Materials Processing Technology 115(1). 2001;44–48.

[45] Rosochowski A, Presz W, Olejnik L, Richert M. Mint: Microextrusion of ultra-fine grained aluminium. International Journal of Advanced Manufacturing Technology 33(1–2). 2007;137–146.

[46] Egerer E, Engel U. Mint: Process characterization and material flow in microforming at elevated temperatures. Journal of Manufacturing Processes 6 (1). 2004;1–6.